IOPscience iopscience.iop.org

Home Search Collections Journals About Contact us My IOPscience

Measuring and modeling absolute data for electron-induced processes

This content has been downloaded from IOPscience. Please scroll down to see the full text.

2012 J. Phys.: Conf. Ser. 388 012001

(http://iopscience.iop.org/1742-6596/388/1/012001)

View the table of contents for this issue, or go to the journal homepage for more

Download details:

IP Address: 134.21.16.139
This content was downloaded on 22/10/2014 at 14:01

Please note that terms and conditions apply.

XXVII International Conference on Photonic, Electronic and Atomic Collisions (ICPEAC 2011) IOP Publishing
Journal of Physics: Conference Series **388** (2012) 012001 doi:10.1088/1742-6596/388/1/012001

Measuring and modeling absolute data for electron-induced processes

Michael Allan

Department of Chemistry, University of Fribourg, Chemin du Musée 9, 1700 Fribourg, Switzerland

E-mail: Michael.Allan@unifr.ch

Abstract. This article draws a connecting line between a number of publications scattered in the literature with the aim of making some general conclusions. Emphasis is on dissociative electron attachment (DAE), since this process leads to chemical change, essential for many applications. Four domains of phenomena involved in DEA are identified: threshold or 'nonlocal' phenomena, the 'multidimensional' phenomena, the Feshbach resonance domain, and processes where scrambling of atoms occurs. The point is made that these four groups of phenomena are linked in real world, and that a unified theory describing all of them is required.

1. Introduction

This paper gives a somewhat personal retrospective of selected measurements over the past about 20 years which appear particularly interesting to me, with emphasis on work done in Fribourg. Many of the observations were made possible by improved instrumentation, justifying a brief review of instrumental progress. The interplay of experiment and theory for achieving progress will be emphasized. The paper will further point out that four groups of phenomena contribute to electron-driven chemistry, the DEA. An illustrative prototype example of each group will be described and it will be pointed out that theoretical development treating all of them in a unified manner would be very desirable. Last not least this paper is an unofficial homage on George J. Schulz, whose work [1] was decisive for my decision to spend my career studying resonances in electron-molecule collisions.

2. Introduction to resonances: H_2

Since this article addresses also scientists not familiar with the field, the essential points are summarized on the example of H_2, shown schematically in Fig. 1. Three types of resonances are shown: a shape resonance with a single occupation of the normally unoccupied orbital σ_u, a valence-core excited resonance with a hole in the σ_g orbital and a double occupation of the σ_u orbital, and Feshbach resonances with a hole in the σ_g orbital and double occupancy of Rydberg-type orbitals.

The scheme serves as a prototype for many electron-induced processes which will be found also in the more complicated molecules discussed below. Electron scattering can generally be understood as a vertical electron attachment, followed by relaxation of the nuclei as indicated for the shape resonance in the bottom part of the figure. If the electron detaches in early stages of the relaxation, then elastic scattering or vibrational excitation result. Vibrational

Published under licence by IOP Publishing Ltd

excitation cross section is thus a valuable means of obtaining experimental information on resonances. If the electron detaches in later stages of relaxation, then it leads to excitation of high vibrational levels. That means that electron scattering may be looked at as a crudely time-resolved experiment where longer time delays are measured *via* excitation of high vibrational levels. The part of the wave packet which survives till the stabilization point leads to dissociative electron attachment (DEA). The competition between detachment and DEA leads to two effects useful for experimental characterization of resonances: (i) the DEA cross section drops rapidly with increasing autodetachment rate, *i.e.*, the resonance width Γ, and (ii) the DEA isotope effect, in this case the cross section ratio $\sigma(H_2)/\sigma(D_2)$, rises rapidly with increasing Γ and becomes thus an experimental measure of the resonance autodetachment width. The isotope effect is 200 in H_2, revealing a very large Γ. The DEA cross section is also useful means of experimentally studying resonances, but, as indicated in Fig. 1, the band shapes may be different in DEA and VE. The DEA band is cut-off on the low-energy side by the threshold, and drops fast on the high-energy side because Γ rises with decreasing R and increasing energy.

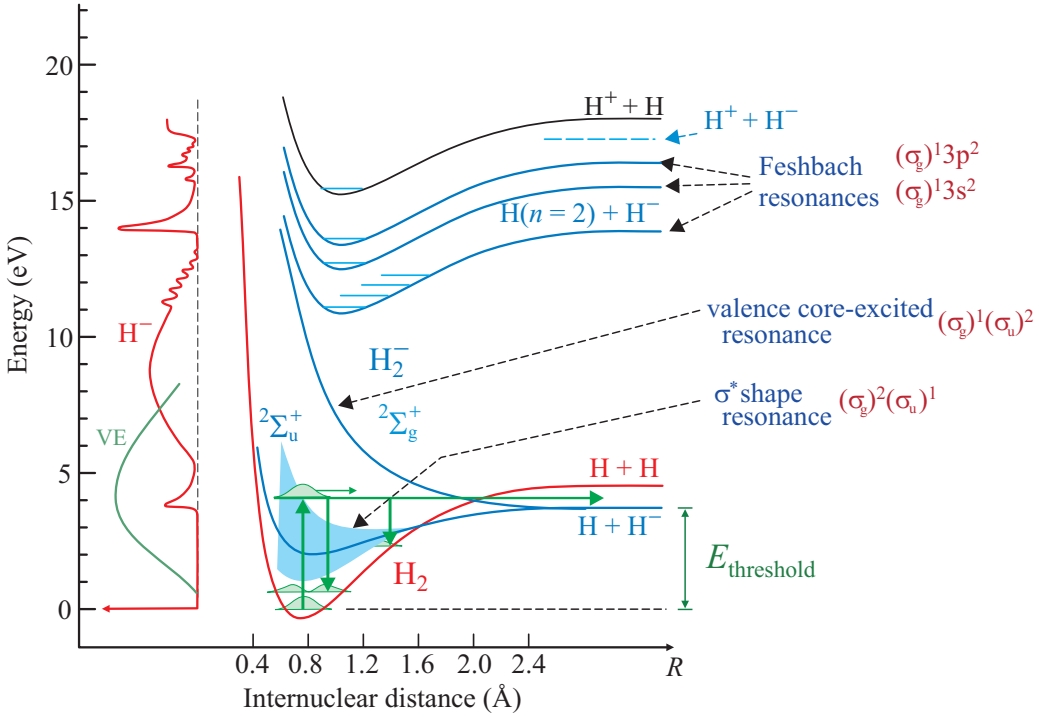

Figure 1. Selected schematic potential surfaces of H_2, H_2^- and H_2^+. Schematic spectra of vibrational excitation (VE) and dissociative electron attachment (DEA) are shown on the left.

A valence core-excited resonance (repulsive in the case of H_2) is found at higher energy and is observed as a broad DEA band. VE is not a suitable means to study it experimentally because the attachment cross section for the two-electron process is low. The relatively narrow width (the experimentally observed wide band is dominated by the wide Frank-Condon envelope) makes it important for DEA, however. It is an important prototype, because valence core excited resonances of this type are responsible for DEA in many polyatomic molecules. At still higher energies many Feshbach resonances with double occupation of Rydberg-like orbitals are found. They arise in series converging to the 1st, 2nd, etc. ionization energies. Nominally, the two outer electrons are in spatially diffuse orbitals, with very little density between the atoms, and affect chemical binding very little. The potential surface of the Feshbach resonances consequently

resembles that of the cation to which they converge, and which is, at least for ground state ion, not repulsive – so naive expectation is that the Feshbach resonances do not contribute to DEA. In reality, however, the Feshbach resonances are often predissociated by repulsive anion states, and give rise to intense DEA bands. This is the case for H_2 – manifested by the sharp structures shown schematically in the DEA spectrum in the 11-13 eV range – and also in many polyatomic molecules as will be shown below on the example of CH_3OH.

3. Instruments

In the late '70s when I entered the electron collision field as a postdoc in the group of George Schulz at Yale university the field was very exciting, in particular the study of resonances [1], but I was frustrated by instrumental deficiencies which prevented many interesting measurements:
- The electron spectrometers suffered from large background, which prevented measurements of small cross sections.
- The cross sections could be measured only over limited energy ranges - the focusing voltages of the electrostatic lenses are a strongly nonlinear functions of the electron energy - they were approximated by a linear function and this approximation was valid only over a narrow energy range.
- It was very difficult to reach energies below 1-2 eV; slow electrons were lost because of inhomogeneities of surface potentials and of weak residual magnetic fields.
- Although methods for measuring absolute cross sections for elastic, inelastic, and dissociative attachment cross section existed at the time, the majority of published data was only relative, and substantial discrepancies were often found between the absolute values measured in different laboratories.
- The angular range was limited, often between about 20° and 120°.
- As shown above on the example of H_2, competing decay channels provide mutually complementary information on the resonances and it is thus very instructive for the understanding to have a "complete study", that is, absolute cross sections for all processes (elastic, vibrational and electronic excitation, DEA).

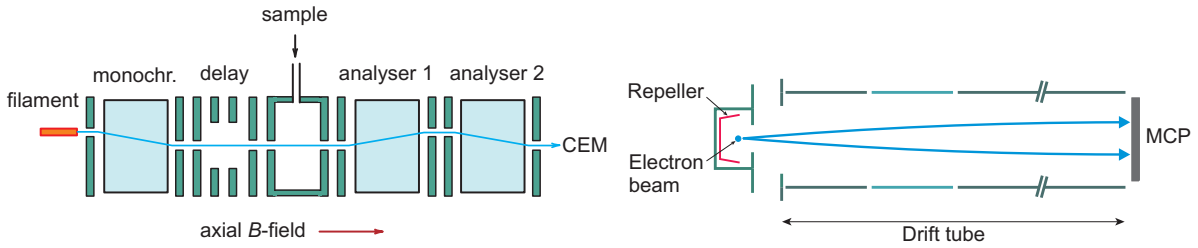

Figure 2. Left: Scheme of the electron energy-loss spectrometer with trochoidal analyzers. Right: Scheme of the Time-Of-Flight mass spectrometer for absolute DEA cross sections.

It was my ambition in Fribourg to remove these limitations by improving the instrumentation, and to use the new instruments for a deeper study of electron collisions and of resonances. Parallel efforts for instrumental development took place at other laboratories, of course, in particular in United Kingdom, Australia, Austria, Germany, Japan, Korea, United States.

The first instrument constructed in Fribourg was a magnetically collimated spectrometer with trochoidal analyzers (TES), shown schematically on the left of Fig. 2 [2]. This instrument was very sensitive and permitted measurements of small cross sections, for example for high vibrational levels or for electronic excitation. It could not measure absolute cross sections and angular distributions, however, and was later replaced by a spectrometer with hemispherical

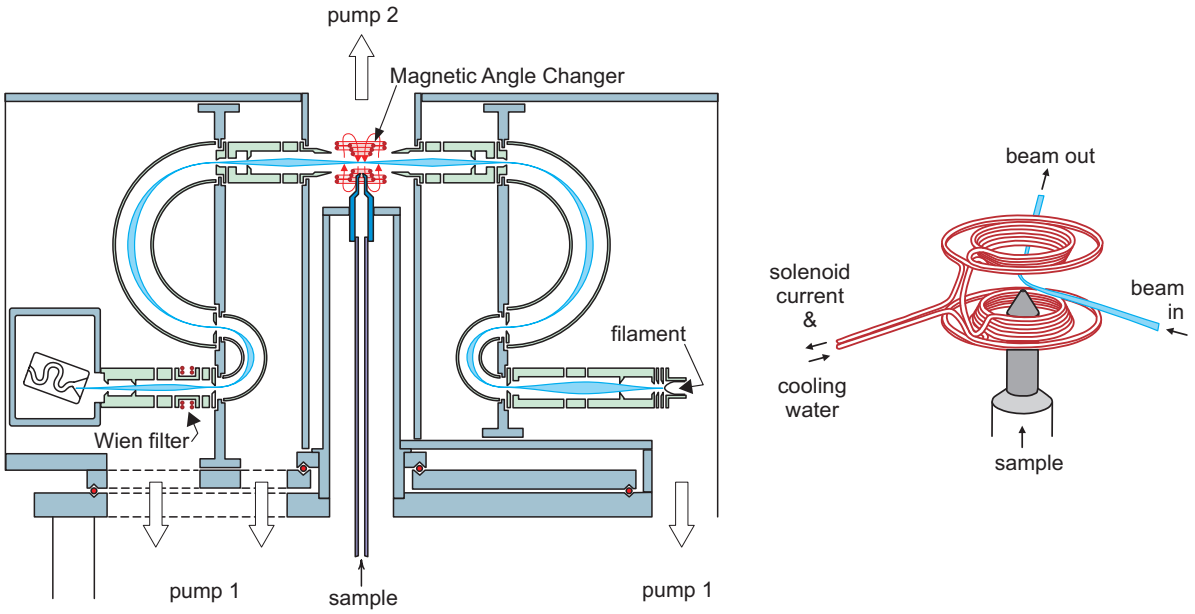

Figure 3. Scheme of the electron energy-loss spectrometer with hemispherical analyzers. Detail of the magnetic angle changer is shown on the right.

analyzers, shown schematically in Fig. 3 [3–5]. This instrument is slightly less sensitive than the TES, but is superior in the sense that it allows measurements of absolute cross sections and angular distributions. The instrument greatly benefited from the invention of the Magnetic Angle Changer (MAC) by Read and Channing [6, 7]. The Fribourg version is wound from few turns of water-cooled copper tubing and has the advantage of only minimal interference with gas flow. A small Wien filter separates scattered electrons and negative ions from DEA when necessary. The instrument can thus also measure DEA, under high resolution, and with angular distribution and resolution of product ion energies [8]. It is limited to relatively large DEA cross sections in this mode, however.

The latest addition to the instrumental park in Fribourg is a Time-Of-flight (TOF) mass spectrometer optimized for the measurements of absolute cross sections [9], and which was attached at 90° to the modified target chamber of the TES.

4. Excitation of high vibrational levels in H_2

As already pointed out in connection with Fig. 1, the lowest shape resonance in H_2 has an autodetachment width much broader than vibrational spacing and the cross sections for exciting $v = 1$ and $v = 2$ have no vibrational structure. It was initially theoretical work [10] which indicated that structure of vibrational origin (albeit lifetime-broadened – called boomerang structure) may appear in the cross sections for excitation of higher vibrational levels. These cross sections are very small, however, and it required the very high sensitivity of the TES instrument to measure them [11], with the result shown in Fig. 4.

A qualitative explanation of the seeming contradiction between the extreme Γ and the presence of vibrational structure is indicated by the potential curves on the right in Fig. 4. (It is based on the theoretical work [10, 12] and numerous patient explanations by the theoreticians.) For boomerang structure to appear, one needs an interference of an outgoing and an incoming wave [13, 14], the latter being reflected by the far wing of the potential, where the anion is bound. But in H_2 the wave packet diminishes very rapidly initially, so that the reflected wave

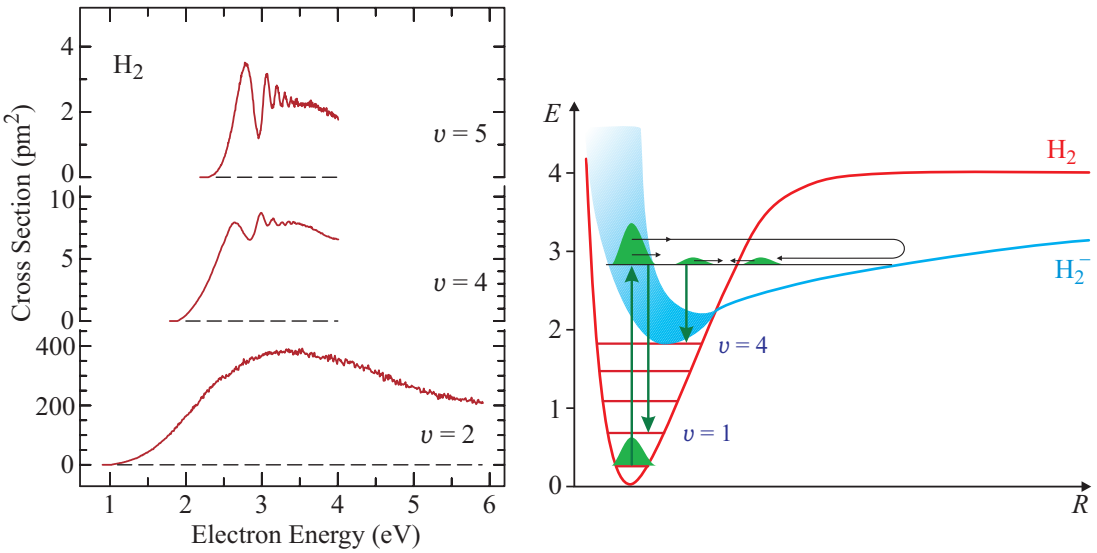

Figure 4. Cross sections for vibrational excitation of H_2 and schematic potential curves.

packet has a very small amplitude. At R where a vertical downward transition leads to $v = 1$ (or $v = 2$) excitation, there is a dramatic mismatch of the outgoing and incoming wave amplitudes, with no noticeable interference. At larger R, where a vertical transition leads to $v = 4$ and higher excitation, the outgoing wave has already greatly decayed, outgoing and incoming wave amplitudes match, and interference gives rise to oscillatory structures in the cross section.

The lesson to be learned is that cross sections for the excitation of high vibrational levels are very interesting: they represent experimental means to look at greater time delays and there is an increased chance to observe oscillations, which bear information about the outer, 'chemical', wing of the potential curve – which is otherwise hard to observe because it is far from the Franck-Condon region. ('chemical' because it leads to the 'chemical' channel – DEA) This lesson will be used further below, for halogen hydrides, CO_2 and N_2O.

The quest for extending resonance lifetime by including nuclear motion has been driven to the extreme by Čížek, Horáček and Domcke [15] who have predicted theoretically that in suitable high rotational levels the H_2^- resonance, with nominally fs autodetachment lifetime, can live ms (for D_2^-). The prediction was later verified experimentally.

5. Threshold phenomena

More detailed account and extensive literature references can be found in a review article [16]. The threshold phenomena will be illustrated on HF, where Vibrational Feshbach Resonances (VFR) (originally called nuclear-excited resonances) were first positively experimentally identified [17]. Fig. 5 is based on the refined experimental results and potential curves of Ref. [18].

5.1. HF

HF has a σ^* orbital not unlike that of H_2 and one would therefore expect a very broad σ^* resonance and a broad hump in the VE cross section, like that for $v = 2$ in H_2 in Fig. 4. The reality, shown on the left of Fig. 5, is dramatically different in two respects:

- the VE cross sections do not start with a nearly zero value like in H_2, but have a threshold peak and
- there are sharp structures at low energies (around 1 and 1.4 eV) even in the $v = 1$ and

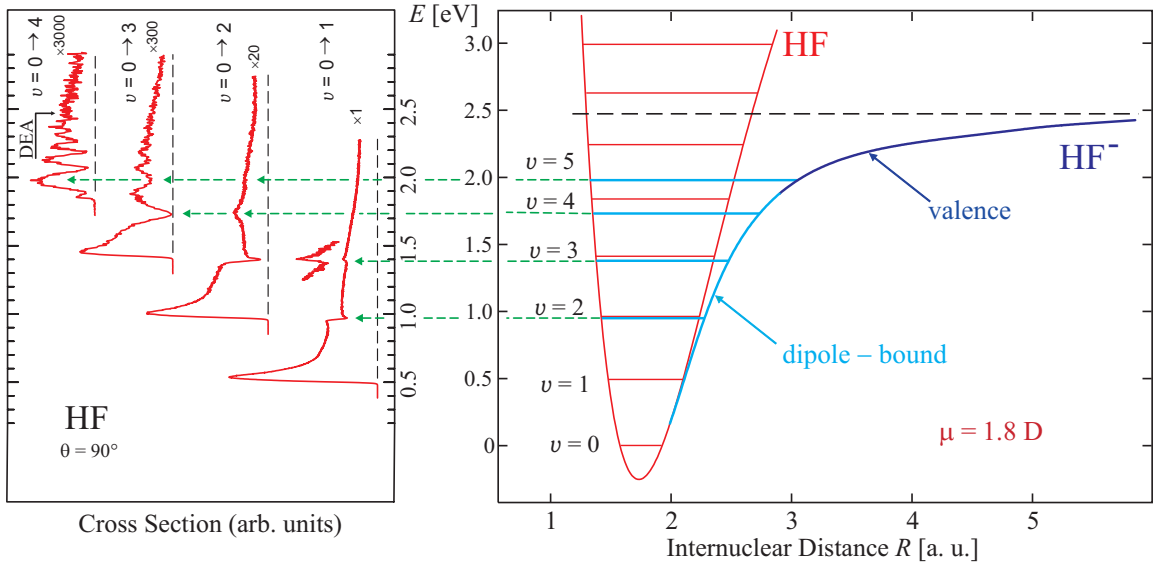

Figure 5. Left: Cross sections for vibrational excitation of HF. Right: Schematic potential curves with vibrational levels of HF and VFR of HF^- indicated.

$v = 2$ cross sections. At higher energies (above about 1.8 eV) and for higher final v, there are oscillations like in H_2.

The explanation lies in the fact that HF has a dipole moment, which is not sufficient to bind an electron at equilibrium internuclear distance but increases with internuclear distance such that HF becomes capable of binding an extra electron (at the fixed nuclei picture) at R slightly larger than the equilibrium internuclear distance. This dipole-bound potential curve then merges, through an avoided crossing, with the valence σ^* potential curve analogous to that of H_2^-. The result is that the σ^* potential curve does not bent up with decreasing R like in H_2, but bends down. The dipole-bound part of the potential curve supports narrow VFRs manifested as sharp structures in the VE cross sections, just below the parent vibrational levels of HF. The energy separation of the parent vibrational levels and the VFRs increases with increasing energy and at the same time they become broader. At still higher energy they become oscillatory structures entirely analogous to those in H_2 – the nuclear wave packet is now reflected on the valence part of the anion potential curve, not the dipole bound part.

These oscillatory structures are visible only in the higher final channels like in H_2 and they converge, also like in H_2, to the DEA limit. Note another subtle similarity: the sign (dip or peak) of the oscillations alternates as the final vibrational quantum number is incremented, *i.e.*, when there is a dip in the cross section for a given final v, like at 2 eV in the $v = 0 \rightarrow 3$ cross section, there is a peak at the same energy for the next final v, like in the $v = 0 \rightarrow 4$ cross section.

Note that the HF^- changes character dramatically as R is varied; it is valence, with a tight wave function, at larger R and becomes dipole-bound, with a spatially large wave function, at shorter R, and completely unbound at even shorter R. How is it possible that the HF^- "potential well", with its left wall missing, is capable of supporting narrow VFR? A qualitative explanation (due to Jean-Pierre Gauyacq) is the following: As the nuclei vibrate, they bind the electron cloud at larger internuclear distances. When they arrive at short R, the electron is in principle (adiabatically) allowed to leave, but it departs only slowly because it has a low energy. That is, before the electron cloud can depart completely, the nuclei return to larger internuclear separation where a portion of the departing electron cloud is re-captured – permitting several

oscillations of the nuclei before the extra electron is entirely lost. A qualitative explanation for the threshold peaks is that the VFR, although nominally below the vibrational threshold, also extend to energies at and above the threshold. This high-energy tail of the VFR is responsible for the large VE cross section just above threshold.

Subtle phenomena concerning the oscillatory structures deserve to be mentioned here – they cause two types of superimposed structures to occur instead of just one oscillatory structure. An "outer well" may form in the potential curve of the anion when the valence part of the curve has (with decreasing R) a minimum before bending down, like in HCl [19]. This gives rise to "outer well resonances", causing narrow structures superimposed on the wavy oscillatory structure. A second type of structure, superimposed on the oscillations, may be found even in cases where no clear outer well occurs in the potential curve, as has been particularly clearly pointed out theoretically by Houfek *et al.* [20]. They lead to irregularities and odd shapes in VE cross sections, like in NO [21].

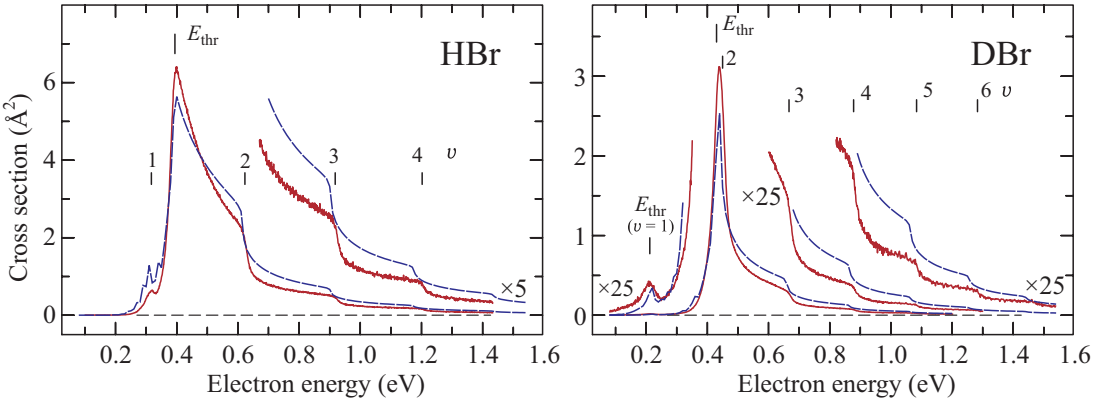

Figure 6. Theoretical (dashed lines) and experimental absolute dissociative electron attachment cross sections of HBr and DBr [22, 23].

5.2. HBr

The dipole (and polarizability) binding and the ensuing bending-down of the potential curve, and the 'nonlocal effects' related to it, cause threshold peaks and oscillatory structures in VE cross sections below the DEA threshold, but they also have an effect above the threshold, on DEA. This is illustrated on HBr in Fig. 6. The important features are: (i) The cross section is very large at threshold and (ii) there are pronounced downward steps in DEA at thresholds for VE. The downward steps were first observed in Orsay [24] and can be understood as a drop of the 'quantum flux' into the DEA channel when a competing VE channel opens up. The theoretical description requires nonlocal formalism and Fig. 6 illustrates the impressive success of the Prague/Munich version of the nonlocal resonance theory both in terms of shape and in terms of absolute magnitude of the spectra. Similar success was recently achieved for HCl [25]. An alternative and very successful approach is that of R-matrix theory, applied in Lincoln [26].

HBr serves as a prototype of a very general phenomenon in acidic molecules. Weak downward steps were observed and theoretically rationalized in formic acid [27] and more pronounced steps were predicted [26] and observed [28] in aminoacids. The mechanism is active even in the nucleic base uracil [29].

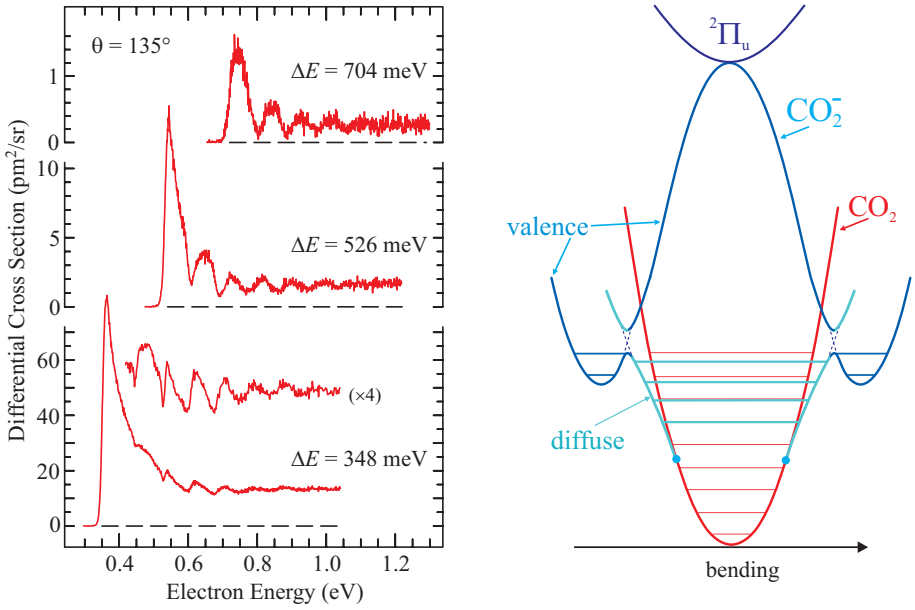

Figure 7. Left: Cross sections for exciting the topmost members of the Fermi polyads around 2, 3 and 4 quanta of the symmetric stretch vibration [30]. Right: Hypothetical potential curves.

5.3. CO_2

CO_2 is another case where the improved resolution and sensitivity were a necessary prerequisite for new observations, related to Fermi-coupled vibrations, which are only about 12 meV apart, and because small cross sections for excitation of high vibrational levels must be measured. Vibrational excitation in CO_2 is dominated by a $^2\Pi_u$ π^* resonance around 3.8 eV [31] and by a threshold peak ascribed to a virtual state. High resolution experiments revealed a dramatic selectivity in the virtual state domain – only the topmost member of each polyad of Fermi-coupled vibrations (where symmetric stretch ν_1 and even quanta of bending ν_2 mix) are excited. When the 'lesson' from H_2 (sec. 4) was applied, and high vibrational levels were measured, then structure appeared in the virtual state region as shown in Fig. 7 [30]. The structure is remarkably similar to that of HF (Fig. 5), suggesting that it has the same physical origin. The explanation is illustrated by the hypothetical potential curves in Fig. 7. The spacing of the experimental structures indicates that the bending coordinate is relevant. When CO_2 is bent, then it acquires temporarily a dipole moment which, together with the polarizability binding responsible for the virtual state, yields a 'bound' potential surface, supporting VFRs, much like in HF. The diffuse state is linked to the valence state of bent CO_2^- through avoided crossing. The structure was reproduced theoretically [32] and interesting physical insight about the remarkable preference for the highest member of each Fermi-polyad issued from this study.

CO_2 is a prototype case showing that the threshold phenomena encountered in HF and HBr are not limited to molecules with dipole moment and are encountered more frequently than initially suspected.

6. Multidimensional phenomena

6.1. Chlorobenzene

Breaking of a given bond in a polyatomic molecule *via* a shape resonance is often hindered by an energy barrier which can be by-passed by symmetry lowering and a suitable distortion of the molecular framework. The theoretical description can then not be treated as a quasi one

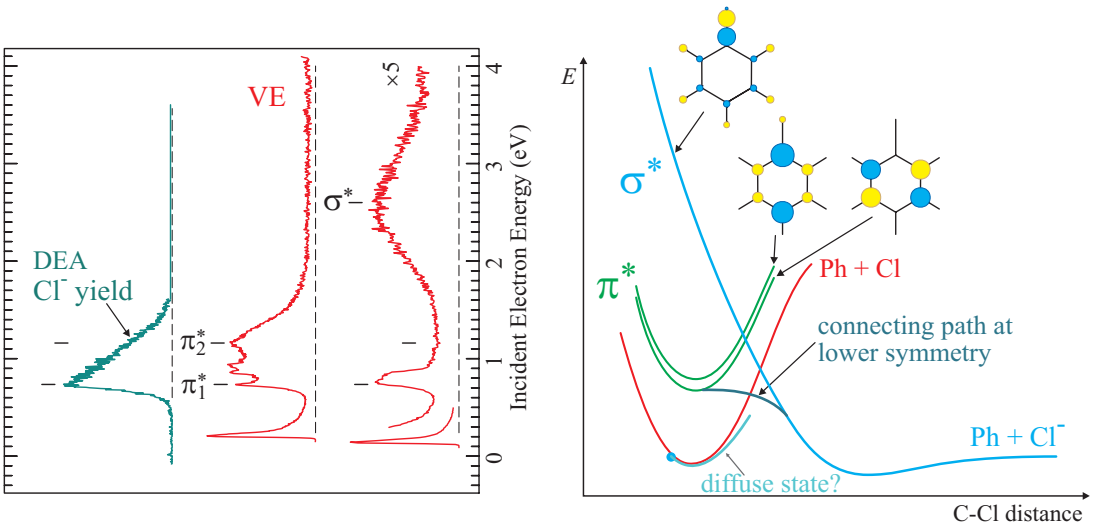

Figure 8. Left: Cross sections for exciting the C−Cl stretch (bottom) and the ring breathing (center) vibrations, and the DEA (Cl^- yield) spectrum [33]. Right: Hypothetical potential curves.

dimensional problem but several dimensions must be included explicitly. An illustrative example is chlorobenzene as shown in Fig 8. The VE cross sections on the left reveal two overlapping π^* resonances around 1 eV and a broad σ^* resonance around 2.6 eV. The σ^* resonance is assigned as such because it excites selectively the C−Cl stretch and not the ring breathing vibrations. A naive expectation for DEA is a broad Cl^- band around 2.6 eV, caused by the σ^* resonance, repulsive along the C−Cl bond, and no Cl^- yield at 1 eV because the π^* resonances are not dissociative along the C−Cl bond. Exactly the opposite is observed: Cl^- signal has a vertical onset at the energy of the $v = 0$ level of the π^* resonance, there is no activation barrier. The barrier has been proposed to be lowered by a distortion, primarily bending of the C−Cl bond out of the plane of the benzene ring (causing conjugation of the π^* and σ^* orbitals) and twisting of the benzene ring [33]. The σ^* resonance has an autodetachment width too large for DEA.

The symmetry-lowering can be described as a consequence of vibronic coupling, which has been considered also for resonances [34–36]. An unanswered question is whether dipole-bound states similar to those discussed above for HF and HBr are involved. The threshold peaks in the VE cross sections in Fig 8 may be an indication of such states, but no sharp structures similar to those in HF and CO_2 were observed.

6.2. Acetylene and hydrogen cyanide

Acetylene is an important prototype case because absolute DEA cross sections were calculated *ab-initio* taking into account three dimensions explicitly [37]. The theoretical cross sections were validated by comparison with experimental absolute cross sections and satisfactory agreement was found both for the absolute values and the isotope effect [9, 38, 39]. The theory calculated *ab-initio* the local complex potential for the lowest resonance, followed by time-dependent dynamics of a nuclear wave packet on this potential. It provided a detailed insight into the DEA mechanism by showing how the energy barrier present at linear geometry is dramatically lowered by bending the C−H bond, until it disappears around 30°.

Hydrogen cyanide has been calculated by the same formalism and satisfactory agreement with experiment was found, although slightly less good than for acetylene [40, 41]. The insight provided by the nuclear dynamics is somewhat surprising – although barrier to dissociation,

lowered by C−H bending, was found like in the acetylene case, the preferred mechanism was tunneling of the nuclear wave packet through the barrier and not going around it. HCN is more acidic than acetylene and the question arises whether the 'nonlocal' mechanism for which HBr is a prototype does not also contribute to DEA.

6.3. Formic acid

Formic acid has a π^* resonance which has a barrier along the O−H dissociation path which can be by-passed by suitable molecular distortion and in this sense is a candidate for the 'multidimensional' DEA mechanism for which chlorobenzene and acetylene are prototypes [42, 43]. At the same time it is acidic and in this sense a viable candidate for the 'HBr mechanism' [44, 45]. The *R*-matrix study predicted the downward steps which were observed experimentally [27, 46]. More light into this question will be shed by measurements of absolute cross sections of deuterated isotopomers [47].

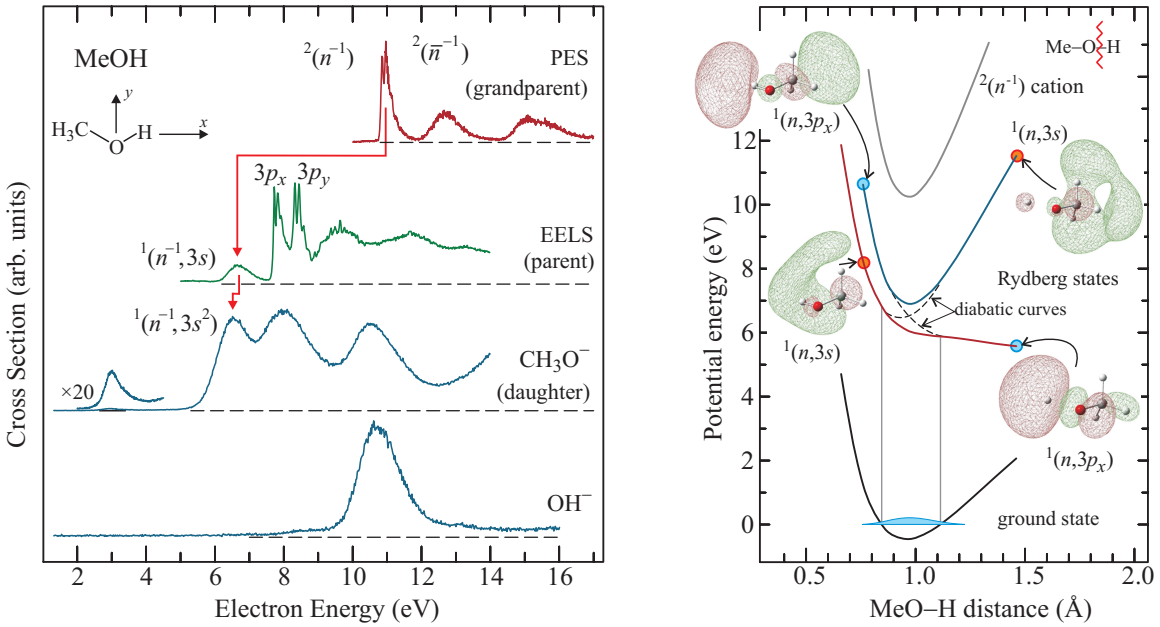

Figure 9. Left: Photoelectron spectrum (top), EELS spectrum, and two DEA spectra showing the relation between the grandparent cation, parent Rydberg and daughter Feshbach resonances in methanol. The absence of C−O bond breaking by the lowest Feshbach resonance $^2(n^{-1}, 3s^2)$ is shown at the bottom. Right: Potential curves of the ground state, the two lowest Rydberg states, and the lowest cation state of methanol [48, 49].

7. Core excited resonances

Large DEA cross sections are often encountered in the 5-15 eV range and methanol will be briefly presented here as a prototype example [48, 49]. The spectra for two representative fragments are shown in Fig. 9. The prominent CH_3O^- band at 6.53 eV can be assigned as the lowest Feshbach resonance with a hole in the highest occupied MO, the lone pair n, and two electrons in diffuse $3s$ Rydberg-like orbitals, *i.e.* as $^2(n^{-1}, 3s^2)$. The assignment is based on the well known energetic relation between the grandparent cation, the parent Rydberg, and the daughter Feshbach resonance states [50–53], as illustrated in Fig. 9. The enigma is the same as already described for H_2 in section 2: The grandparent cation state is not dissociative and the two $3s$

electrons are mostly outside of the molecules, not contributing significantly to bonding – the Feshbach resonance would not be expected to dissociate.

This enigma is present already in the parent Rydberg state with one $3s$ electron, as manifested by the lack of vibrational structure in the $^1(n^{-1}, 3s)$ lowest EELS band – in contrast to the sharp vibrational structure in the $^2(n^{-1}$ cationic state and the $^1(n^{-1}, 3p)$ states. This lack of structure is caused by a repulsive potential surface, as has been recognized, in the case of water, already early, by G. Herzberg [54]. We therefore decided – not having the theoretical means to calculate the potential surfaces of the Feshbach resonances – to to gain insight into the dissociative mechanism by calculating the potential surfaces of the Rydberg states, as shown for the O−H dissociation on the right of Fig. 9. The results rationalize the observations, they show that the $^1(n^{-1}, 3s)$ rapidly changes its nature when the O−H bond is stretched, acquiring some $3p$ nature by avoided crossing and then shrinking in size and becoming a repulsive σ^* state. This theoretical treatment also rationalized an important experimental finding, that the $^2(n^{-1}, 3s^2)$ resonance breaks the O−H bond and not the C−O bond [49]. It should be mentioned that these observations and conclusions are not limited to methanol, but apply to all the alcohols and ethers studied in Fribourg.

8. Complex chemistry

DEA in polyatomic molecules sometimes leads to fragments whose structure bears little resemblance to the structure of the target – several bonds need to be broken, new bonds formed, "scrambling" occurs. This represents an enigma in the sense that such complex rearrangement cannot happen on the fs-ps timescale defined by autodetachment. An older example of DEA to methyl acetate [55] is mentioned here as a prototype, although many impressive examples were found more recently by the Innsbruck and Berlin groups.

The explanation of the enigma is that the resonance is stabilized by rapid relaxation to reach sections of the anion potential surface where anion is more stable than the neutral, *e.g.*, forms a hot stable anion which detaches only very slow electrons on a timescale much longer than the original vertically formed resonance. The complex chemistry occurs within this metastable anion, on the bound part of the potential. The metastable anion can be the parent anion or a fragment resulting from rapid initial fragmentation. In the case of methyl acetate a qualitative potential surface was proposed based on the observed fragments and their thermochemistry [55].

Another interesting example is the electron-induced intermolecular proton transfer in the formic acid dimer, identified by the large yield of very slow electrons from the hot product anion [56]. The proton-transferred species was also identified by anion photoelectron spectroscopy [57]. The theoretical treatment of these reactions does not require scattering calculations in the bound part of the potential surface, advanced quantum-chemical methods are amendable [58].

9. Conclusions

This article identifies four domains of phenomena involved in dissociative electron attachment. They are illustrated in the generic diagram in Fig. 10 and are:
(a) The threshold or 'nonlocal' phenomena, where HBr is the prototype case. They require long range binding of an electron by a permanent dipole or by polarizability. This results in a potential curve which bends down with decreasing interatomic distance (instead of rising as a very broad σ^* resonance like in H_2) and the resulting well supports Vibrational Feshbach Resonances. Thought initially to be a rare exotic phenomenon, it is now recognized to be important in many biomolecules [26].
(b) The 'multidimensional' phenomena, which require that several dimensions of motion of the nuclei are taken into account and which cannot be reduced to a diatomic or quasi-diatomic model. The prototype cases are chlorobenzene and acetylene.

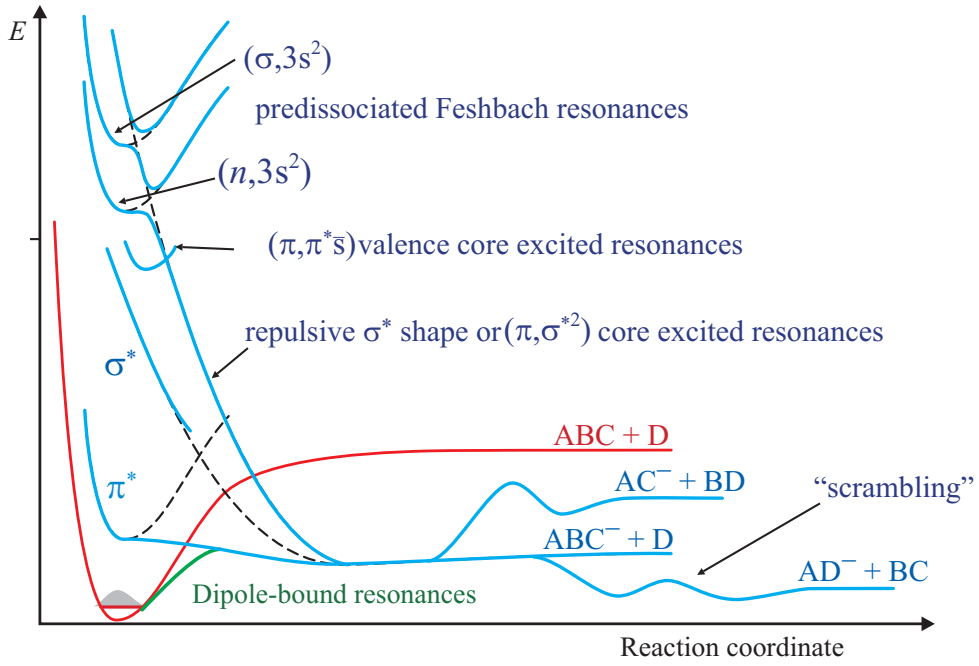

Figure 10. Generic potential curves involved in dissociative electron attachment. Neutral target is shown in red, various states of the negative ion in blue, the dipole bound state green. Diabatic curves are dashed.

(c) Higher energy (>5 eV) phenomena dominated by core excited Feshbach resonances and where predissociation by repulsive single particle or core excited states is essential. The prototype case is methanol. Related to this group are DEA bands coinciding with the lowest valence excited state, normally in unsaturated compound, and assigned to en electron weakly bound to the valence excited state, *i.e.*, $^2(\pi, \pi^*\bar{s})$.
(d) Processes where substantial chemical change occurs on areas of the potential surface where the anion is bound.

Doorway states are common, where a nominally non-dissociative but narrow resonance serves as an entrance channel and is predissociated by a repulsive (σ^*) state which autodetaches too fast in the vertical attachment point to cause DEA by itself, but whose width decreases rapidly with increasing bond lengths, making it important for predissociation. At present, several theoretical methods exist which specialize in one or another of these domains, but in reality they are intertwined and one of the great challenges for theory is developing models treating several of these groups of phenomena in a unified way.

9.1. Acknowledgments

This research is part of project No. 200020-131962/1 of the Swiss National Science Foundation, of project SBF No. C07.0018 of the State Secretariat for Education and Research and of COST Action CM0601.

References

[1] Schulz G J 1973 *Rev. Mod. Phys.* **45** 423
[2] Allan M 1989 *J. Electron Spectrosc. Relat. Phenom.* **48** 219
[3] Allan M 1992 *J. Phys. B: At. Mol. Opt. Phys.* **25** 1559
[4] Allan M 2005 *J. Phys. B: At. Mol. Opt. Phys.* **38** 3655–3672

[5] Allan M 2010 *Phys. Rev. A* **81** 042706/1–042706/9
[6] Read F H and Channing J M 1996 *Rev. Sci. Instrum.* **67** 2373
[7] Zubek M, Gulley N, King G C and Read F H 1996 *J. Phys. B: At. Mol. Opt. Phys.* **29** L239
[8] Allan M 2004 *J. Phys. B: At. Mol. Opt. Phys.* **37** L359–L363
[9] May O, Fedor J and Allan M 2009 *Phys. Rev. A* **80** 012706
[10] Mündel C, Berman M and Domcke W 1985 *Phys. Rev. A* **32** 181–193
[11] Allan M 1985 *J. Phys. B* **18** L451
[12] Horáček J, Čížek M, Houfek K, Kolorenč P and Domcke W 2006 *Phys. Rev. A* **73** 022701
[13] Birtwistle D T and Herzenberg A 1971 *J. Phys. B* **4**(1) 53–70
[14] Dubé L and Herzenberg A 1979 *Phys. Rev. A* **20** 194–213
[15] Čížek M, Horáček J and Domcke W 2007 *Phys. Rev. A* **75** 012507
[16] Hotop H, Ruf M W, Allan M and Fabrikant I I 2003 *Adv. At. Mol. Opt. Phys.* **49** 85
[17] Knoth G, Gote M, Rädle M, Jung K and Ehrhardt H 1989 *Phys. Rev. Lett.* **62** 1735–1737
[18] Čížek M, Horáček J, Allan M, Fabrikant I I and Domcke W 2003 *J. Phys. B* **36** 2837–2849
[19] Allan M, Čížek M, Horáček J and Domcke W 2000 *J. Phys. B: At. Mol. Opt. Phys.* **33** L209
[20] Houfek K, Čížek M, Jiří and Horáček 2008 *Chem. Phys.* **347** 250–256
[21] Allan M 2005 *J. Phys. B: At. Mol. Opt. Phys.* **38** 603
[22] Fedor J, May O and Allan M 2008 *Phys. Rev. A* **78** 032701
[23] Horáček J, Čížek M, Kolorenč P and Domcke W 2005 *Eur. Phys. J. D* **35** 255–230
[24] Abouaf R and Teillet-Billy D 1977 *J. Phys. B: At. Mol. Phys.* **10** 2261–2268
[25] Fedor J, Winstead C, McKoy V, Čížek M, Houfek K, Kolorenč P and Horáček J 2010 *Phys. Rev. A* **81** 042702
[26] Fabrikant I I 2010 *J. Phys. Conf. Ser.* **204** 012004
[27] Pelc A, Sailer W, Scheier P, Mason N and Märk T 2002 *Eur. Phys. J. D* **20**(3) 441–444
[28] Vizcaino V, Bartl P, Gschliesser D, Huber S E, Probst M, Märk T D, Scheier P and Denifl S 2011 *ChemPhysChem* **12** 1272–1279
[29] Gallup G A and Fabrikant I I 2011 *Phys. Rev. A* **83** 012706
[30] Allan M 2002 *J. Phys. B: At. Mol. Opt. Phys.* **35** L387
[31] Boness M J W and Schulz G J 1974 *Phys. Rev. A* **9** 1969–1979
[32] Vanroose W, Zhang Z, McCurdy C W and Rescigno T N 2004 *Phys. Rev. Lett.* **92** 053201
[33] Skalický T, Chollet C, Pasquier N and Allan M 2002 *Phys. Chem. Chem. Phys.* **4** 3583
[34] Estrada H, Cederbaum L S and Domcke W 1986 *J. Chem. Phys.* **84** 152
[35] Gallup G A 1993 *J. Chem. Phys.* **99** 827–835
[36] Feuerbacher S, Sommerfeld T and Cederbaum L 2004 *J. Chem. Phys.* **120**(7) 3201–3214
[37] Chourou S T and Orel A E 2008 *Phys. Rev. A* **77** 042709
[38] Chourou S T and Orel A E 2009 *Phys. Rev. A* **80** 034701
[39] Azria R and Fiquet-Fayard F 1972 *J. Physique* **33** 663–667
[40] Chourou S T and Orel A E 2011 *Phys. Rev. A* **83** 032709
[41] May O, Kubala D and Allan M 2010 *Phys. Rev. A* **82** 010701
[42] Rescigno T N, Trevisan C S and Orel A E 2006 *Phys. Rev. Lett.* **96** 213201
[43] Rescigno T N, Trevisan C S and Orel A E 2009 *Phys. Rev. A* **80** 046701
[44] Gallup G A, Burrow P D and Fabrikant I I 2009 *Phys. Rev. A* **79** 042701
[45] Gallup G A, Burrow P D and Fabrikant I I 2009 *Phys. Rev. A* **80** 046702
[46] Pelc A, Sailer W, Scheier P, Probst M, Mason N J, Illenberger E and Märk T D 2002 *Chem. Phys. Lett.* **361** 277–284
[47] Kubala D, May O and Allan M 2011 in preparation
[48] Ibănescu B C, May O, Monney A and Allan M 2007 *Phys. Chem. Chem. Phys.* **9** 3163–3173
[49] Ibanescu B C and Allan M 2008 *Phys. Chem. Chem. Phys.* **10** 5232–5237
[50] Sanche L and Schulz G J 1972 *Phys. Rev. A* **6** 69
[51] Sanche L and Schulz G J 1973 *J. Chem. Phys.* **58** 479–493
[52] Skalický T and Allan M 2004 *J. Phys. B* **37** 4849
[53] Khvostenko V I and Pogulay A V 1992 *Organic Mass Spectr.* **27** 681–685
[54] Goodeve C F and Stein N O 1931 *Trans. Farad. Soc.* **21** 393–404
[55] Pariat Y and Allan M 1991 *Int. J. of Mass Spectrom. and Ion Proc.* **103** 181
[56] Allan M 2007 *Phys. Rev. Lett.* **98** 123201
[57] Ko Y J, Wang H, Radisic D, Stokes S T, Eustis S N, Bowen K H, Mazurkiewicz K, Storoniak P, Kowalczyk A, Haranczyk M, Gutowski M and Rak J 2010 *Mol. Phys.* **108**(19) 2621–2631
[58] Bachorz R A, Haranczyk M, Dabkowska I, Rak J and Gutowski M 2005 *J. Chem. Phys.* **122** 204304